OPEN

Oncogene (2016) **35,** 5963–5976

www.nature.com/onc

ORIGINAL ARTICLE

Inhibition of FOXC2 restores epithelial phenotype and drug sensitivity in prostate cancer cells with stem-cell properties

AN Paranjape[1,10], R Soundararajan[1,10], SJ Werden[1], R Joseph[1], JH Taube[1], H Liu[1], J Rodriguez-Canales[1], N Sphyris[1], I Wistuba[1], N Miura[2], J Dhillon[3], N Mahajan[3], K Mahajan[3], JT Chang[4], M Ittmann[5], SN Maity[6], C Logothetis[6], DG Tang[7] and SA Mani[1,8,9]

Advanced prostate adenocarcinomas enriched in stem-cell features, as well as variant androgen receptor (AR)-negative neuroendocrine (NE)/small-cell prostate cancers are difficult to treat, and account for up to 30% of prostate cancer-related deaths every year. While existing therapies for prostate cancer such as androgen deprivation therapy (ADT), destroy the bulk of the AR-positive cells within the tumor, eradicating this population eventually leads to castration-resistance, owing to the continued survival of $AR^{-/lo}$ stem-like cells. In this study, we identified a critical nexus between p38MAPK signaling, and the transcription factor Forkhead Box Protein C2 (FOXC2) known to promote cancer stem-cells and metastasis. We demonstrate that prostate cancer cells that are insensitive to ADT, as well as high-grade/NE prostate tumors, are characterized by elevated FOXC2, and that targeting FOXC2 using a well-tolerated p38 inhibitor restores epithelial attributes and ADT-sensitivity, and reduces the shedding of circulating tumor cells *in vivo* with significant shrinkage in the tumor mass. This study thus specifies a tangible mechanism to target the $AR^{-/lo}$ population of prostate cancer cells with stem-cell properties.

Oncogene (2016) **35,** 5963–5976; doi:10.1038/onc.2015.498; published online 25 January 2016

INTRODUCTION

Prostate cancer (PCa) progression to metastatic disease accounts for >10% of all cancer-related deaths in men. Androgen deprivation therapy (ADT) remains the principal treatment for PCa. While this results in initial tumor regression, the majority of these patients become noncompliant to this line of treatment, owing to the emergence of androgen-independent mechanisms promoting tumor cell growth. Moreover, although most initially diagnosed PCas are acinar adenocarcinomas that display elevated expression of the androgen receptor (AR) and its target gene prostate-specific antigen (PSA), a substantial proportion of patients present atypical clinical features, and are characterized by the blatant absence of AR and PSA, but instead display immunoreactivity to neuroendocrine (NE) differentiation markers such as chromogranin A, synaptophysin, CD56 and neuron-specific enolase. While these AR/PSA-negative NE PCas (NEPC) (or small-cell prostate carcinomas) are rare at the time of initial diagnosis, they however, account for 10–30% of advanced recurrent castration-resistant PCas (CRPC, high-grade Gleason) following ADT.[1] These variant 'AR-negative PCa' or NEPCs are extremely aggressive, androgen-independent, metastatic and therapy resistant, with their 5-year overall survival being dismal at 12.6%, which categorizes them as the most deadly subset of all PCa.[2] Currently, there are no targeted therapies available for this class of patients; their AR-negativity presents a major therapeutic challenge.

It has long been recognized that androgens and AR exhibit key tumor suppressive effects in the prostate. Genetic ablation of AR in prostate epithelial cells has actually been demonstrated to promote the development of invasive prostate tumors,[3] while targeting AR with siRNA has been shown to promote metastasis through enhanced macrophage recruitment via STAT3 activation.[4] Moreover, AR expression is significantly reduced in metastatic hormone-resistant PCa,[5] while AR signaling was found to be severely attenuated in some advanced PCa.[6] Collectively, this argues that restoration of AR and AR signaling could indeed have beneficial effects for the select class of PCa patients (such as those diagnosed with NEPC/small-cell prostate carcinomas, or even advanced adenocarcinomas displaying NE differentiation following ADT) that feature loss of AR or its downstream molecular targets.

Emerging evidence implicates the existence of a subpopulation of androgen-insensitive stem-like cells in prostate tumors (PCaSCs) that may potentially aid in tumor recurrence, metastatic progression and therapy-resistance.[7–10] However, the origin of these cells and the molecular factors governing their stem-cell behavior are still poorly understood, although there have been suggestions that PCaSCs may be NE in nature (and hence $AR/PSA^{-/lo}$).[11] In a recent report aimed at characterizing the cancer stem-cell (CSC) pool from PCa explants, drug-resistant sphere cultures were found to be particularly enriched for cytokeratin 18, suggesting their epithelial origin.[7] Further, elevated expression of Zeb1, an epithelial-mesenchymal-transition (EMT) transcription factor associated with stem-cell properties, in androgen-independent PCa cells as well as in prostate tumors of castrated PTEN

[1]Department of Translational Molecular Pathology, UT MD Anderson Cancer Center, Houston, TX, USA; [2]Department of Biochemistry, Hamamatsu University School of Medicine, Hamamatsu, Japan; [3]Department of Oncological Sciences, Moffitt Cancer Center, University of South Florida, Tampa, FL, USA; [4]Department of Integrative Biology and Pharmacology, School of Medicine, School of Biomedical Informatics, UT Health Sciences Center at Houston, Houston, TX, USA; [5]Department of Pathology and Immunology, Baylor College of Medicine, Houston, TX, USA; [6]Department of Genitourinary Medical Oncology, UT MD Anderson Cancer Center, Houston, TX, USA; [7]Department of Molecular Carcinogenesis, Science Park, UT MD Anderson Cancer Center, Smithville, TX, USA; [8]Metastasis Research Center, UT MD Anderson Cancer Center, Houston, TX, USA and [9]Center for Stem Cell and Developmental Biology, UT MD Anderson Cancer Center, Houston, TX, USA. Correspondence: Dr SA Mani, Department of Translational Molecular Pathology, UT MD Anderson Cancer Center, 2130 West Holcombe Blvd, LSP9.2001, UTMDACC, Houston, TX 77030, USA.
E-mail: mani@mdanderson.org
[10]These authors are co-first authors.
Received 29 August 2015; revised 4 November 2015; accepted 20 November 2015; published online 25 January 2016

conditional knockout mice advocates that PCaSCs are possibly products of EMT.[12]

EMT refers to a complex cellular reprogramming process that facilitates the conversion of differentiated epithelial cells into loosely organized, highly migratory and invasive mesenchymal cells. Although there are multiple suggestions that deviant activation of EMT pathways may facilitate the development of PCa, and possibly, aid in its progression to the advanced therapy-resistant state,[12–14] the precise molecular mechanisms that dictate the EMT/CSC-mediated shift to altered AR signaling as well as to androgen-independence, and the source of stem-cells in PCa progression, remain largely undefined.

Employing a PSA promoter-driven lentiviral EGFP reporter system, we previously demonstrated that in both primary PCa tissues, and in established PCa cell lines, the $PSA^{-/lo}$ cells represent a functionally unique subpopulation that is selectively enriched for cells characteristic of castration-resistant PCaSC.[15] This undifferentiated pool of cells expresses classical PCaSC markers (ALDH, CD44, α2β1-integrin), and undergoes asymmetric cell division to generate the PSA^{+}/differentiated counterpart of prostate epithelial cells. Further, these cells are endowed with elevated clonogenic potential and tumor-propagating capacity, thereby highlighting the potential clinical benefit of effectively targeting this subpopulation of PCa cells. In a distinct set of studies, we previously identified the central EMT regulator Forkhead Box Protein C2 (FOXC2) as an independent factor necessary and sufficient to bestow carcinoma cells with CSC features, as well as with migratory and invasive capacities required for tumor progression *in vivo*.[16,17]

In this manuscript, we demonstrate a direct link between $PSA^{-/lo}$ PCa cells, the EMT/CSC archetype and regulated AR expression, and establish a vital role for FOXC2 in the induction and maintenance of ADT-resistant PCaSC attributes. Further, we describe the use of a novel approach to target FOXC2 expression/function as an effective method of inhibiting the generation/function of tumor-promoting $PSA^{-/lo}AR^{-/lo}$ stem-like cells, while simultaneously restoring epithelial attributes in these cells, hence resensitizing them to ADT.

RESULTS

$PSA^{-/lo}$ PCa stem-like cells exhibit augmented EMT properties

We have recently shown that the $PSA^{-/lo}$ subpopulation of cells from primary human prostate tumors, as well as from various PCa cell lines, represent self-renewing, tumor-propagating cells resembling PCaSC.[15] We have also previously demonstrated that in breast carcinoma, EMT constitutes a major source for the generation of such tumor-propagating stem-like cells.[17] To investigate the relationship between EMT and PSA, we isolated PSA^{+} and $PSA^{-/lo}$ sub-fractions, from the androgen-responsive LNCaP cell line expressing the PSA promoter driving green fluorescent protein (GFP) expression, as described previously,[15] and analyzed the expression of well-characterized EMT markers. In comparison to the PSA^{+} (GFP^{+}) fraction, the $PSA^{-/lo}$ ($GFP^{-/lo}$) cells clearly appeared more mesenchymal (Figure 1a). Quantitative reverse transcription–PCR (qRT–PCR; Figure 1b) and western blot (Figure 1c) analyses revealed that the stem-like $PSA^{-/lo}$ cells exhibited markedly diminished expression of prostate epithelial differentiation markers AR and PSA, as expected, with simultaneously elevated expression of known stem-cell markers, Bmi1 and Sox2[18] as well as NE differentiation markers [2] (Figure 1b). In addition, $PSA^{-/lo}$ cells also exhibited significantly reduced expression of the epithelial marker E-cadherin, and increased expression of mesenchymal markers and the central EMT regulator, FOXC2 (Figures 1b and c). Immunofluorescent staining further confirmed the loss of expression and plasma membrane localization of E-cadherin, with concomitant increase in expression of CSC markers Zeb1[19,20] and FOXC2 in $PSA^{-/lo}$ cells (Figure 1d). These results suggest that even in the androgen-dependent LNCaP cell line, the $PSA^{-/low}$ cells resembling stem-like cells, display the EMT phenotype as well as NE-like features.

Androgen-independent metastatic PCa cell lines possess increased EMT/stem-cell features

While LNCaP cells are androgen-dependent and poorly invasive, the androgen-independent DU145 and PC3 cells are far more invasive and harbor significantly higher metastatic potential.[21] We observed that LNCaP cells predominantly exhibited epithelial features including expression of AR/PSA and E-cadherin (Figures 1e and f). DU145 and PC3 cells, on the other hand, exhibited significantly increased expression of EMT-associated mesenchymal markers, as well as NE differentiation markers, with simultaneous loss of E-cadherin levels (Figures 1e and f). Interestingly, expression of FOXC2 was restricted to the androgen-independent metastatic cell lines DU145 and PC3, and almost undetectable in the weakly invasive non-metastatic LNCaP cells (Figure 1f).

Since FOXC2 is known to empower tumor cells with stem-cell attributes in breast carcinoma,[17] we tested these PCa cell lines for stem-cell properties including their ability to form prostospheres, and expression of stem-cell-related cell-surface markers CD44 and CD24.[22] In correlation with their reduced sphere-forming capacity in non-adherent cultures, the poorly invasive LNCaP cells harbored $< 1\%$ $CD44^{hi}/CD24^{lo}$ stem-cell-enriched fraction (Figures 1g and h). In contrast, more than 85% of the metastatic DU145 cells were $CD44^{hi}/CD24^{lo}$ (Figures 1g and h), consistent with increased expression of other known stem-cell markers, Bmi1 and Sox2 (Figure 1e). We also observed that the two PCa cell lines expressing high levels of endogenous FOXC2—DU145 and PC3—formed significantly higher number of tumorspheres (Figure 1i), indicating higher stem-like potential compared with LNCaP cells, which have very low FOXC2 expression. Interestingly, the PCa cells that have higher metastatic potential and augmented stem-cell properties consistently lack AR/PSA expression (Figures 1e and f).

FOXC2 expression heralds the androgen-independent state associated with loss of AR/PSA expression, poor Gleason scoring and recurrent PCa

We previously discovered that FOXC2 is not expressed in differentiated breast cancer cells but is markedly upregulated following EMT, and is enriched in CSC fractions.[23] We therefore examined whether induction of EMT in PCa cells would similarly result in upregulation of FOXC2. Indeed, we found that overexpression of Snail or Zeb1 results in induction of EMT and NE trans-differentiation, and most importantly a significant upregulation of FOXC2, with concomitant loss of AR/PSA expression in androgen-dependent LNCaP cells (Figures 2a, c and d). Conversely, inhibition of EMT-inducing genes such as Snail, or Zeb1 in highly metastatic DU145 cells, results in a striking loss of FOXC2 expression or NE-like features, with restoration of AR/PSA expression (Figures 2b, e and f). Collectively, these findings suggest that FOXC2 possibly functions downstream of various EMT pathways in PCa cells.

To further investigate the physiological significance of FOXC2 in prostate tumor progression, we analyzed the GDS4109 GEO database that contains non-recurrent and recurrent PCa samples. Notably, FOXC2 expression was significantly higher in the recurrent samples (Figure 2g). Moreover, we found a direct correlation between markedly increased FOXC2 levels and high Gleason grading, in two independent publicly available data sets (GSE17356 (Figure 2h) and TCGA (Figure 2i)). To confirm the relevance of these observations, we performed immunohistochemistry (IHC) analyses for FOXC2 protein in patient-derived

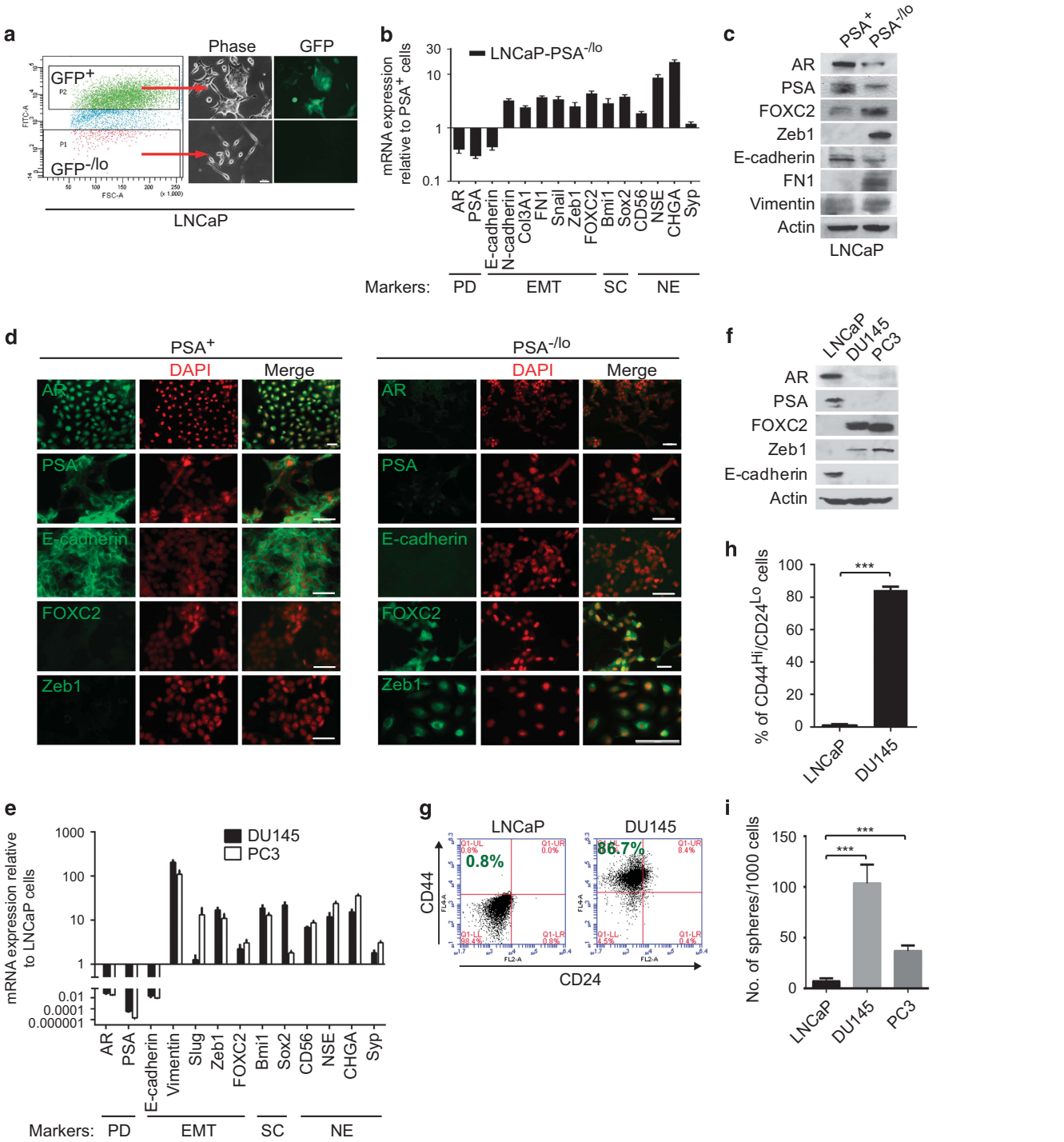

Figure 1. PSA$^{-/lo}$ PCa stem-like cells, as well as androgen-independent PCa cell lines exhibit elevated FOXC2 expression and key properties defining the EMT/CSC phenotype. (**a**) The left panel shows FACS plots representing sorting of GFP^{+} (PSA^{+}) and GFP$^{-/lo}$ (PSA$^{-/lo}$) fractions from LNCaP cells. The right panels show morphology and GFP fluorescence of sorted cells. (**b**) qRT–PCR analyses for FOXC2, and key prostate epithelial differentiation- (PD), neuroendocrine-differentiation- (NE), EMT- and stem-cell (SC)-related markers on sorted PSA^{+} and PSA$^{-/lo}$ fractions from LNCaP cells analyzed immediately after sorting. *Y*-axis represents fold change in HPRT-normalized mRNA expression ($n = 3$; error bars indicate s.e.m.) (**c**) Immunoblotting for FOXC2 and other indicated markers on sorted PSA^{+} and PSA$^{-/lo}$ fractions. (**d**) IF for FOXC2 and indicated markers in sorted PSA^{+} and PSA$^{-/lo}$ cells (scale bar, 100 μm; DAPI: pseudo-colored to red). (**e**) qRT–PCR analyses for FOXC2 and other indicated markers in PC3 and DU145 PCa cells compared with that in LNCaP cells. Y-axis represents fold change in HPRT-normalized mRNA expression compared with that of LNCaP cells ($n = 3$; error bars indicate s.e.m.). (**f**) Immunoblotting for FOXC2 and other indicated markers in the above cells (***$P < 0.001$). (**g**) Representative FACS plots for CD44 (APC) and CD24 (PE) surface marker expression analyzed in LNCaP and DU145 cells. (**h**) Quantification of FACS analysis shown in **d** ($n = 3$; error bars indicate s.e.m.). (**i**) Quantitation of prostospheres ($n = 5$; error bars indicate s.e.m.; ***$P < 0.001$).

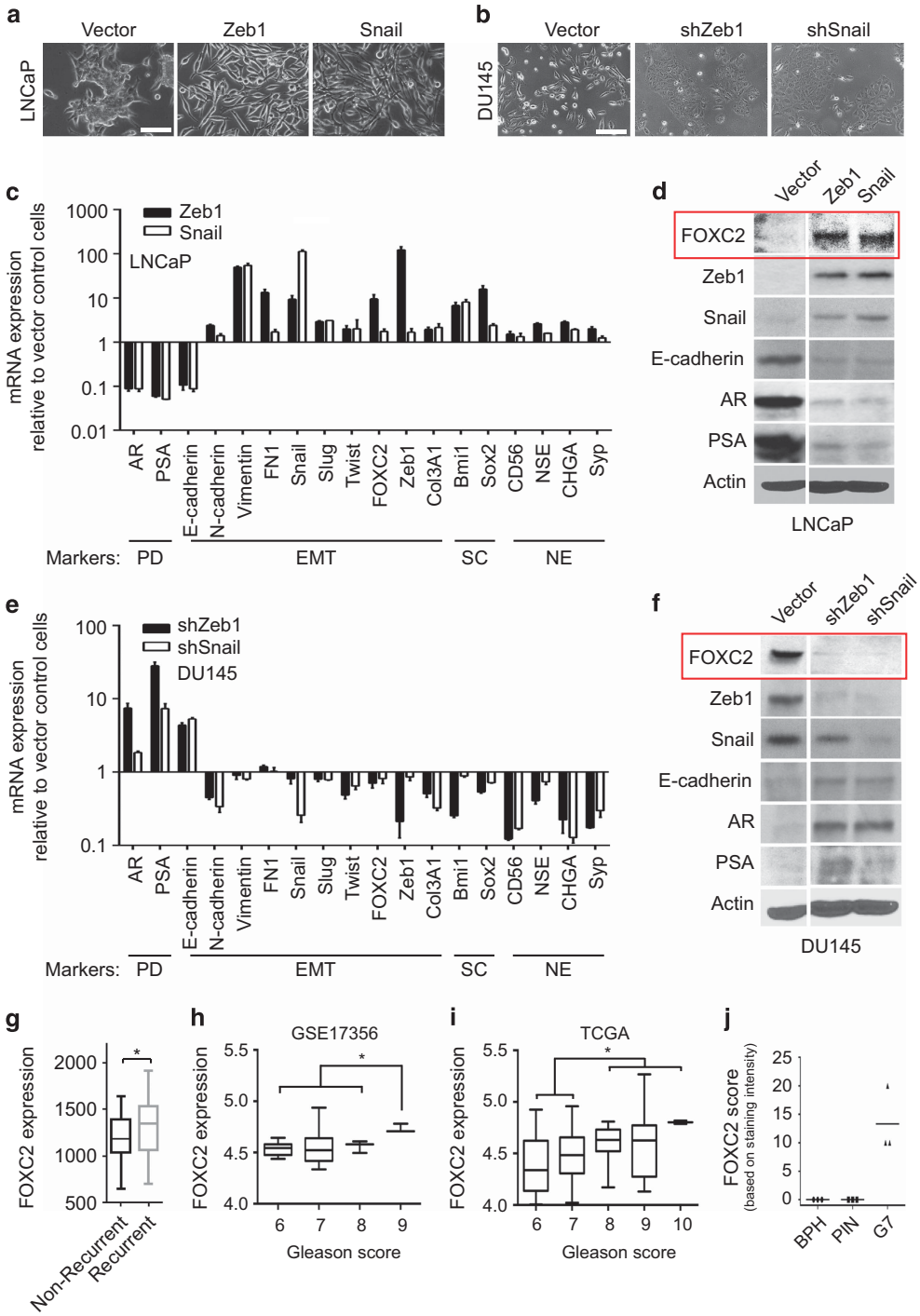

Figure 2. FOXC2 represents a critical convergence factor that is commonly upregulated by multiple EMT inducers in PCa cells, and its expression correlates with recurrent and high Gleason score prostate tumors associated with poor clinical prognosis. (**a**) Morphology of LNCaP cells after stable overexpression of EMT transcription factors—Zeb1 and Snail. (**b**) Morphology of DU145 cells after stable knockdown of Zeb1 and Snail (**a** and **b:** scale bar, 100 μm). (**c** and **e**) qRT–PCR analyses for indicated markers in **a** and **b**, respectively. *Y*-axis represents fold change in HPRT-normalized mRNA expression compared with that of Vector Control cells ($n = 3$; error bars indicate s.e.m.). (**d** and **f**) Immunoblotting for various markers in the indicated cell lines. (**g**) FOXC2 expression levels in recurrent vs non-recurrent clinical PCa data from the GDS4109 GEO database. (**h** and **i**) FOXC2 expression levels in prostate tumors of varying Gleason scores—data from GSE17356 (**h**) and TCGA (**i**) databases. (**j**) Quantitation of FOXC2 protein expression in various patient PCa tissues as analyzed by IHC (corresponding images shown in Supplementary Figure S1; BPH, benign prostatic hyperplasia; G7, Gleason 7); PIN, prostatic intraepithelial neoplasia. *$P < 0.05$.

primary prostate tissue samples ranging from benign prostatic hyperplasia, to prostatic intraepithelial neoplasia, to advanced grade Gleason 7. Interestingly, we discovered a correlation between high expression of FOXC2 and high Gleason grading associated poor clinical outcome (Figure 2j, Supplementary Figure S1), reaffirming our earlier observations. Further, in aggressive small-cell carcinoma of the human prostate characterized by lack of AR, we observed significantly elevated expression

of FOXC2 (Supplementary Figure S2). Similarly, in patient-derived xenograft models of human prostate tumors exemplified by castration-resistance, NE features and loss of AR,[24,25] we consistently observed increased FOXC2 expression (Supplementary Figure S3). Together, these data suggest that expression of FOXC2 in PCa cells segregates with the androgen-independent state that is associated with increased stemness.

Enforced expression of FOXC2 induces the EMT/CSC phenotype and increased drug-resistance

Since FOXC2 is induced downstream of several different EMT inducers, and is by itself capable of potentiating the effects of multiple independent EMT signals,[17,26] we queried how ectopic expression of FOXC2 would impact the behavior of epithelial-like LNCaP cells, which are androgen dependent. In fact, overexpression of FOXC2 resulted in the generation of cells that displayed the classic mesenchymal phenotype (Figure 3a, upper panel) and induced the expression of EMT markers (Figures 3b and c), along with significant upregulation of known stem-cell markers, Bmi1 and Sox2 (Figure 3b), as well as common clinical NE markers (Figure 3b). This was also accompanied by a significant increase in tumorsphere formation (Figure 3d), suggesting enhanced stem-cell function. Again, FOXC2-induced EMT was associated with a reduction in PSA promoter activity (as determined by loss of GFP) (Figure 3a, lower panel), as well as loss of AR expression (Figures 3b and c). We also observed that FOXC2 expression rendered androgen-dependent LNCaP cells increasingly resistant to Enzalutamide (Figure 3e) (a common anti-androgen) and Docetaxel (Figure 3f) (a common chemotherapeutic used in PCa), using the MTS cell survival assay.

Inhibition of FOXC2 reduces stem-cell properties, and restores AR/PSA expression as well as drug sensitivity

To confirm the contribution of FOXC2-mediated EMT in the generation and maintenance of stem-cell attributes in PCa cells, we stably knocked down FOXC2 expression in androgen-independent DU145 cells, which we have shown (Figure 1) to contain a significantly high stem-cell-enriched fraction. Loss of FOXC2 expression resulted in the acquisition of a uniform epithelial phenotype in DU145 cells, which are otherwise known to possess a heterogeneous morphology (Figure 3g), as well as reversal of EMT and NE-like features (Figures 3h and i). Interestingly, we observed a significant upregulation in AR/PSA levels when FOXC2 expression was lost (Figures 3h and j). This was accompanied by a massive reduction in self-renewal potential and stem-cell properties in DU145 cells (Figures 3k–m), including expression of Bmi1 and Sox2 (Figure 3h). DU145 cells are androgen-independent and insensitive to the AR inhibitor Enzalutamide, even at 10 μM.[27] However, suppression of FOXC2 in these cells rendered them more sensitive to Enzalutamide even at 100 nM, as determined by the MTS cell survival assay (Figure 3n).

Emergence of Docetaxel-resistance in PCa remains an important therapeutic hurdle, and DU145 cells represent a good model system to study mechanisms altering Docetaxel-resistance.[28] Interestingly, loss of FOXC2 expression rendered DU145 cells more susceptible to 100 nM Docetaxel treatment (Figure 3o). Together, these results suggest that FOXC2 expression is necessary and sufficient for the induction of PCaSC attributes associated with loss of AR/PSA expression and emergence of androgen-independence and chemo-resistance.

FOXC2 regulates AR via Zeb1, a known transcriptional repressor

It is notable that although FOXC2 functions as a transcriptional activator in most cell types studied, its expression in PCa cells, however, causes a drastic loss of AR/PSA levels. In this context, it is pertinent to reveal parallel studies from our laboratory performed in breast cancer cells, which demonstrate that FOXC2 exerts its repressive effects indirectly through Zeb1, a known transcriptional repressor (Werden *et al.,* under review). We therefore investigated if similar links are operative in PCa cells. In LNCaP cells overexpressing FOXC2, we observed that enforced loss of Zeb1 drastically obliterates the AR-repressive effect of FOXC2 (Figure 4a), as well as their stem-cell properties (Figure 4b), and resistance to Enzalutamide (Figure 4c). Further, overexpression of Zeb1 in DU145 cells lacking FOXC2 expression was sufficient to cause a significant downregulation in AR levels (Figure 4d), with restoration of sphere-forming capacity (Figure 4e) and resistance to Enzalutamide (Figure 4f). These data suggest that FOXC2-dictated PCaSC attributes associated with loss of AR expression and emergence of ADT-resistance are mediated by Zeb1.

Activation of p38MAPK signaling correlates with FOXC2-associated EMT/stem-cell features

p38 mitogen-activated protein kinases (MAPK) are known to play key roles in cellular proliferation, differentiation, apoptosis, invasion and migration—attributes that are all significantly altered during the course of cancer progression.[29] In a parallel study using breast cancer cells, we found that FOXC2 not only possesses functional phosphorylation sites for p38MAPK14, but that both FOXC2 and the active form of p38 (phospho-p38) are consistently high in cells that have undergone EMT, as well as in CSC-enriched cell populations (Werden *et al.,* under review). In fact, we observed that PCa cells with inherent mesenchymal and stem-cell properties (DU145/PC3 relative to LNCaP or PSA^{hi} relative to $PSA^{-/lo}$) exhibit significantly increased p-p38 and its direct target, Activating Transcription Factor-2 (pATF2) (Figures 5a and d), which strongly correlates with FOXC2 expression (Figures 1b, f and 5c, d).

We further tested this correlation between FOXC2 expression and p38 activation in yet another model of prostate EMT induction, using Transforming Growth Factor-β1 (TGFβ1). TGFβ1 is a well-characterized activator of p38 signaling, and has been shown to induce EMT in a variety of epithelial cell types including the prostate.[29,30] Treatment of LNCaP cells with TGFβ1 resulted in moderate induction of EMT, FOXC2 expression, as well as concurrent activation of p38 signaling (Figure 5e), and increased stem-cell function (Figure 5f). On the contrary, suppression of TGFβ1 signaling in DU145 cells using LY364947, resulted in a concomitant loss of FOXC2 expression and p38 signaling (Figure 5e), with markedly reduced tumorsphere-forming capacity (Figure 5f). Together, all the above data suggest that targeting FOXC2, by interfering with p38 signaling, may provide a therapeutic solution to preventing CSC generation/function in androgen-insensitive PCa cells.

Interestingly, we discovered a potential p38 phosphorylation site harbored within a consensus sequence on human FOXC2 protein (Figure 5g). We next investigated the functional relevance of this putative site in facilitating FOXC2-mediated stem-cell functions in PCa cells. While expression of the S367E-FOXC2 mutant, which mimics constitutive p38 phosphorylation, enhanced sphere formation and Zeb1 expression associated with loss of AR, the S367A-FOXC2 mutant, which represents the non-p38-phophorylatable form of FOXC2, resulted in a loss of stem-cell function and Zeb1 expression, with concomitant restoration in AR expression (Figures 5h and i). These results suggest that FOXC2 may be a direct target of p38 in PCa cells, and further that the S367 site plays a key role in mediating FOXC2 functions in these cells.

Suppression of p38 signaling results in reversal of EMT and significant decrease in stem-cell properties

Treatment of DU145 cells with SB203580, a specific chemical inhibitor of p38 signaling, for 7 days resulted in their acquisition of

an epithelial phenotype (Figure 6a), with significant reduction in migratory potential (Figures 6b and c). This was accompanied by a dramatic loss of FOXC2 expression and consequent EMT/CSC features (Figures 6d and e), including significant reduction in the $CD44^{hi}/CD24^{lo}$ fraction (Figures 6f and g), expression of Bmi1 and Sox2 (Figure 6d), and tumorsphere formation (Figure 6h).

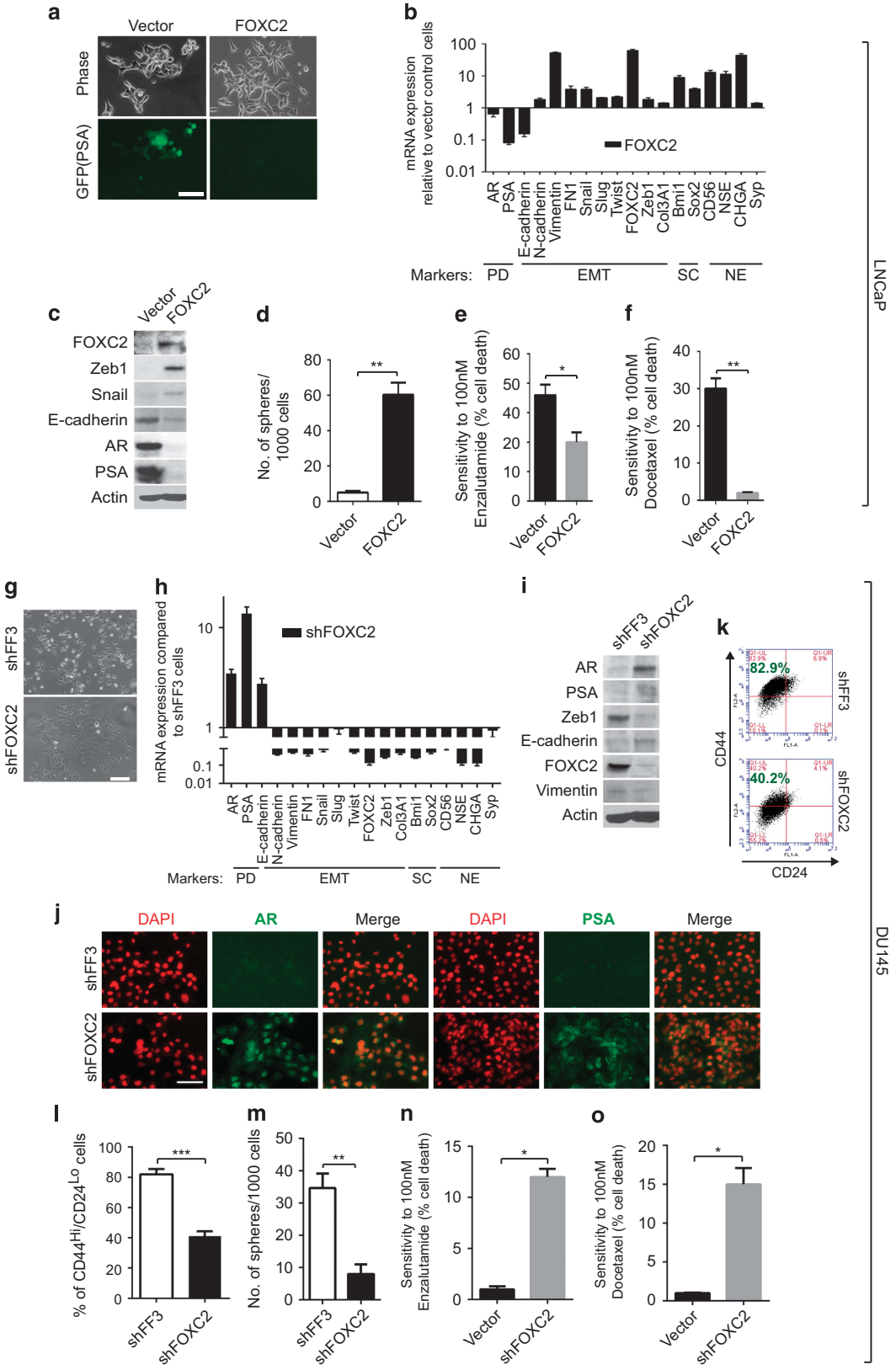

Interestingly, inhibition of p38 signaling and FOXC2 expression using SB203580 resulted in restoration of AR and PSA expression in DU145 cells (Figures 6d, e and i). qRT–PCR performed progressively from days 0–7 after SB203580 treatment revealed that expression of AR, PSA and E-cadherin consistently increased right after 48 h, but reached highest levels at day 7 (Supplementary Figure S4). Interestingly, such restoration of AR/PSA expression with simultaneous loss of FOXC2 brought about by SB203580 pre-treatment, significantly resensitized these cells to subsequent co-treatment with SB203580 and either Enzalutamide (Figure 6j) or Docetaxel (Figure 6k), suggesting that a combinatorial approach might be effective in targeting highly invasive PCa cells that are resistant to ADT and standard chemotherapy.

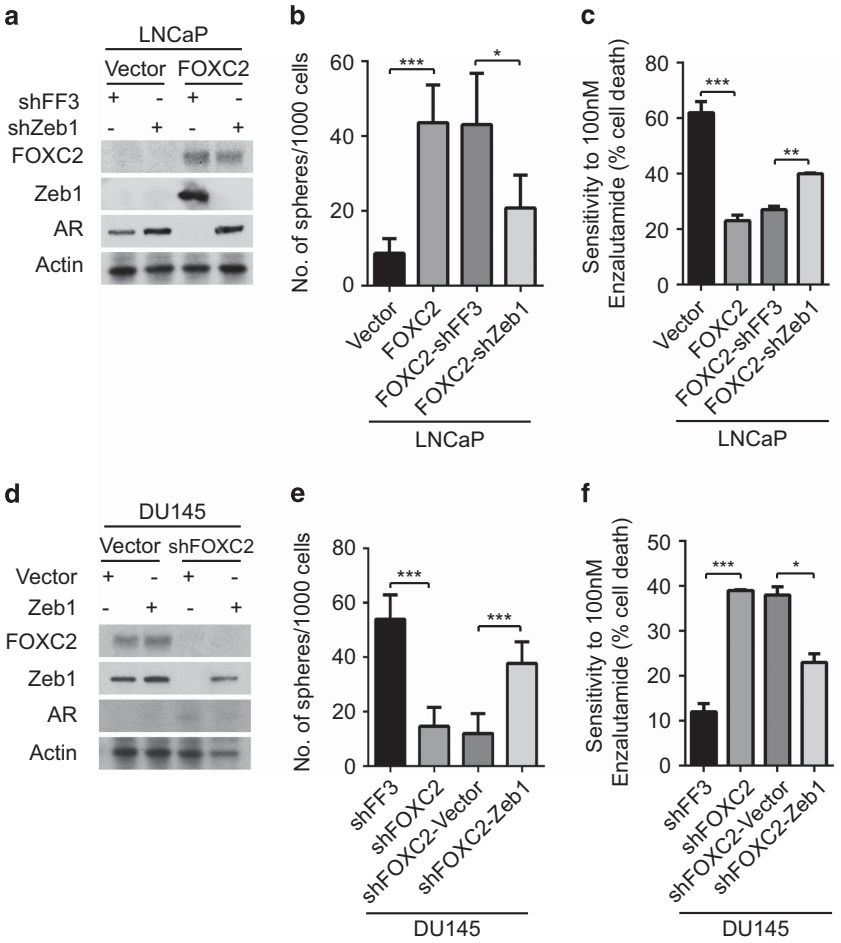

Figure 4. FOXC2 regulates AR expression and stem-cell properties in PCa cells via Zeb1. (**a**) Immunoblotting in LNCaP cells expressing indicated constructs. (**b**) Quantitation of the number of tumorspheres formed per 1000 LNCaP cells, each expressing indicated constructs ($n = 5$; error bars indicate s.e.m.; $^{*}P < 0.05$, $^{***}P < 0.001$). (**c**) Quantification of cell survival using MTS Assay in various LNCaP-derived lines treated with Enzalutamide. Data are represented as absorbance (OD) at 490 nm ($n = 3$), $^{**}P < 0.01$. (**d**) Immunoblotting for Zeb1, FOXC2, AR and Actin in DU145 cells expressing indicated constructs. (**e**) Quantitation of prostospheres formed per 1000 DU145 cells each expressing indicated constructs ($n = 5$; error bars indicate s.e.m.; $^{**}P < 0.001$). (**f**) Quantification of cell survival using MTS Assay in various DU145-derived cell lines treated with Enzalutamide. Data are represented as absorbance (OD) at 490 nm ($n = 3$), $^{*}P < 0.05$, $^{***}P < 0.001$.

Figure 3. FOXC2 is necessary and sufficient to confer EMT/CSC features, and the shift to androgen-independence/drug-resistance in PCa cells. (**a**) The upper panel shows morphology of LNCaP cells after FOXC2 overexpression; the lower panel shows reduction in PSA expression (in the same field) as inferred by reduced expression of GFP cloned downstream of the PSA promoter (scale bar, 100 μm). (**b**) qRT–PCR analyses for indicated markers. *Y*-axis represents fold change in HPRT-normalized mRNA expression compared with that of Vector Control cells ($n = 3$; error bars indicate s.e.m.). (**c**) Immunoblotting for various markers in the indicated cell lines. (**d**) Quantitation of prostospheres ($n = 5$; error bars indicate s.e.m.; $^{**}P < 0.01$). (**e** and **f**) Quantification of cell survival using MTS Assay in FOXC2-overexpressing LNCaP cells treated with Enzalutamide (**e**) or Docetaxel (**f**). Data are represented as absorbance (OD) at 490nm ($n = 3$), $^{*}P < 0.05$, $^{**}P < 0.01$. (**g**) Morphology of indicated cell types (scale bar,100 μm). (**h**) qRT–PCR analyses for indicated markers in DU145 cells on FOXC2 suppression. *Y*-axis represents fold change in HPRT-normalized mRNA expression compared with DU145-shFF3 cells ($n = 3$; error bars indicate s.e.m.). (**i**) Immunoblotting for various markers in the indicated cell types. (**j**) IF for AR/PSA expression in the indicated cell types (scale bar,100μm, DAPI is pseudo-colored to red). (**k**) Representative FACS plots for CD44 (APC) and CD24 (PE) surface marker expression analyzed in the indicated cell lines. (**l**) Graph shows quantification of FACS analysis shown above ($n = 3$; error bars indicate s.e.m.; $^{***}P < 0.001$). (**m**) Quantitation of prostospheres formed per 1000 DU145 cells on FOXC2 suppression ($n = 5$; error bars indicate s.e.m.; $^{**}P < 0.01$). (**n** and **o**) Quantification of cell survival using MTS Assay in DU145-shFOXC2 cells treated with Enzalutamide (**n**) or Docetaxel (**o**). Data are represented as absorbance (OD) at 490 nm ($n = 3$), $^{*}P < 0.05$.

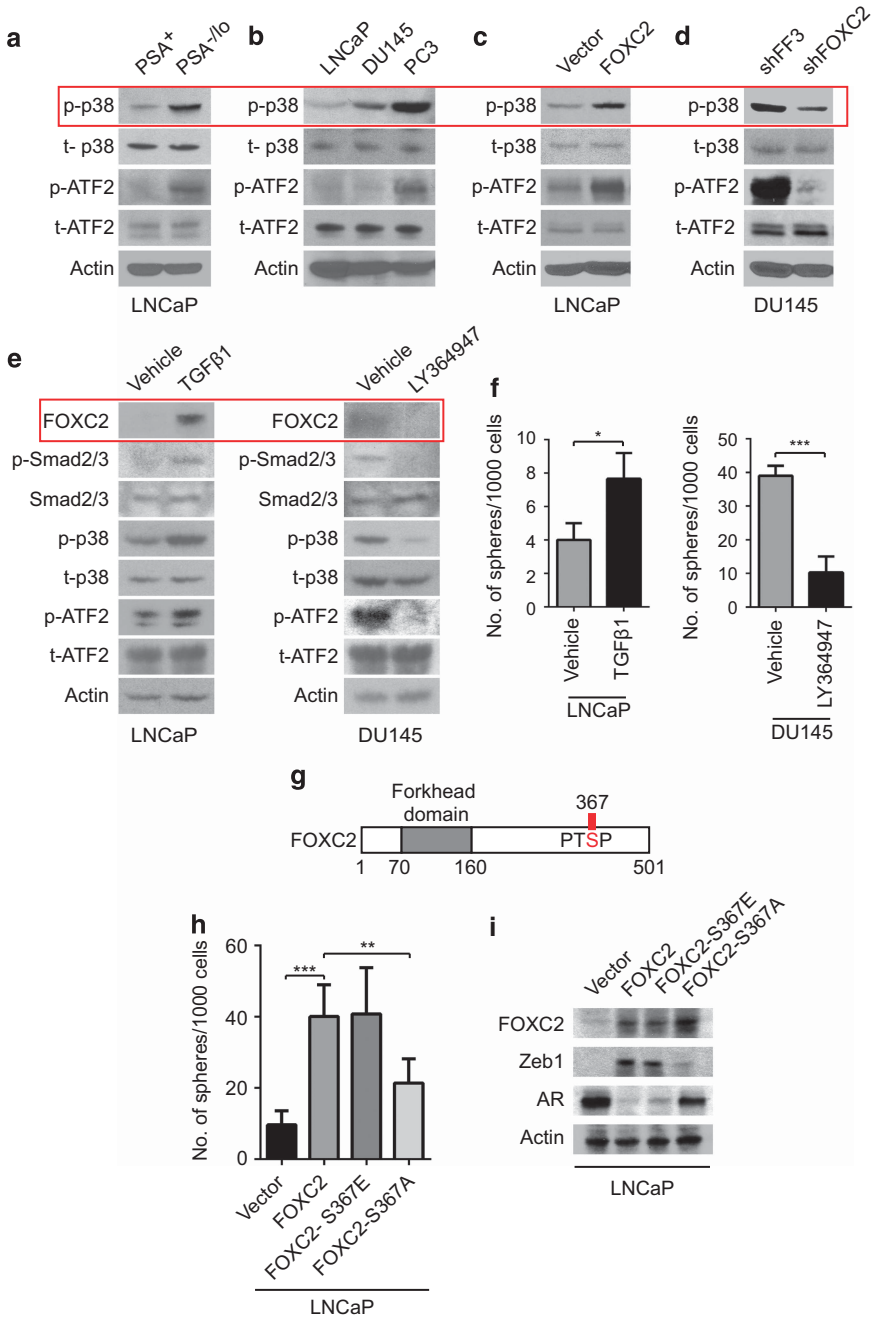

Figure 5. Activation of p38MAPK signaling consistently correlates with the FOXC2-dependent EMT/CSC state in androgen-independent PCa cells. Immunoblotting for total (t)- and phospho (p)-p38 and its target substrate ATF2 in PSA^{+}, $PSA^{-/lo}$ cells (**a**), PCa cell lines (**b**), LNCaP cells after overexpression of FOXC2 (**c**) and DU145 cells after suppression of FOXC2 expression (**d**). (**e**) Immunoblotting for FOXC2, p- and t-Smad2/3 and p38 signaling components in LNCaP cells induced to undergo EMT using TGFβ1 (a physiological activator of p38 signaling), as well as in DU145 cells treated with LY364947, an inhibitor of TGFβ1 signaling. (**f**) Quantitation of tumorspheres ($n = 5$; error bars indicate s.e.m.; $^{*}P < 0.05$, $^{***}P < 0.001$). (**g**) Schematic shows the putative p38MAPK phosphorylation site on human FOXC2 protein based on phospho-motif scan. (**h**) Quantitation of tumorspheres ($n = 5$; error bars indicate s.e.m.; $^{**}P < 0.01$, $^{***}P < 0.001$). (**i**) Immunoblotting in LNCaP cells expressing the indicated constructs.

Combinatorial suppression of p38 signaling with Enzalutamide treatment significantly reduces tumor size

To investigate the effect of inhibition of FOXC2-dependent EMT/CSC attributes on tumor formation *in vivo*, we s.c. injected NOD/SCID mice with DU145 cells and began treatment *in vivo,* after formation of palpable tumors. The treatment plan/schedule is depicted in Figure 7a. While there was no appreciable change in tumor size in mice treated singly with either SB203580 or Enzalutamide compared with the vehicle-treated group, mice treated with a combination of SB203580 and Enzalutamide showed a significant decrease in tumor volume and weight (Figures 7b and e, Supplementary Figure S5). This suggested that although parental DU145 cells are Enzalutamide-resistant to begin with, co-treatment of cells with the p38 inhibitor and Enzalutamide, once again confers susceptibility to ADT. In direct corroboration of our *in vitro* results (Figure 6), such a combinatorial

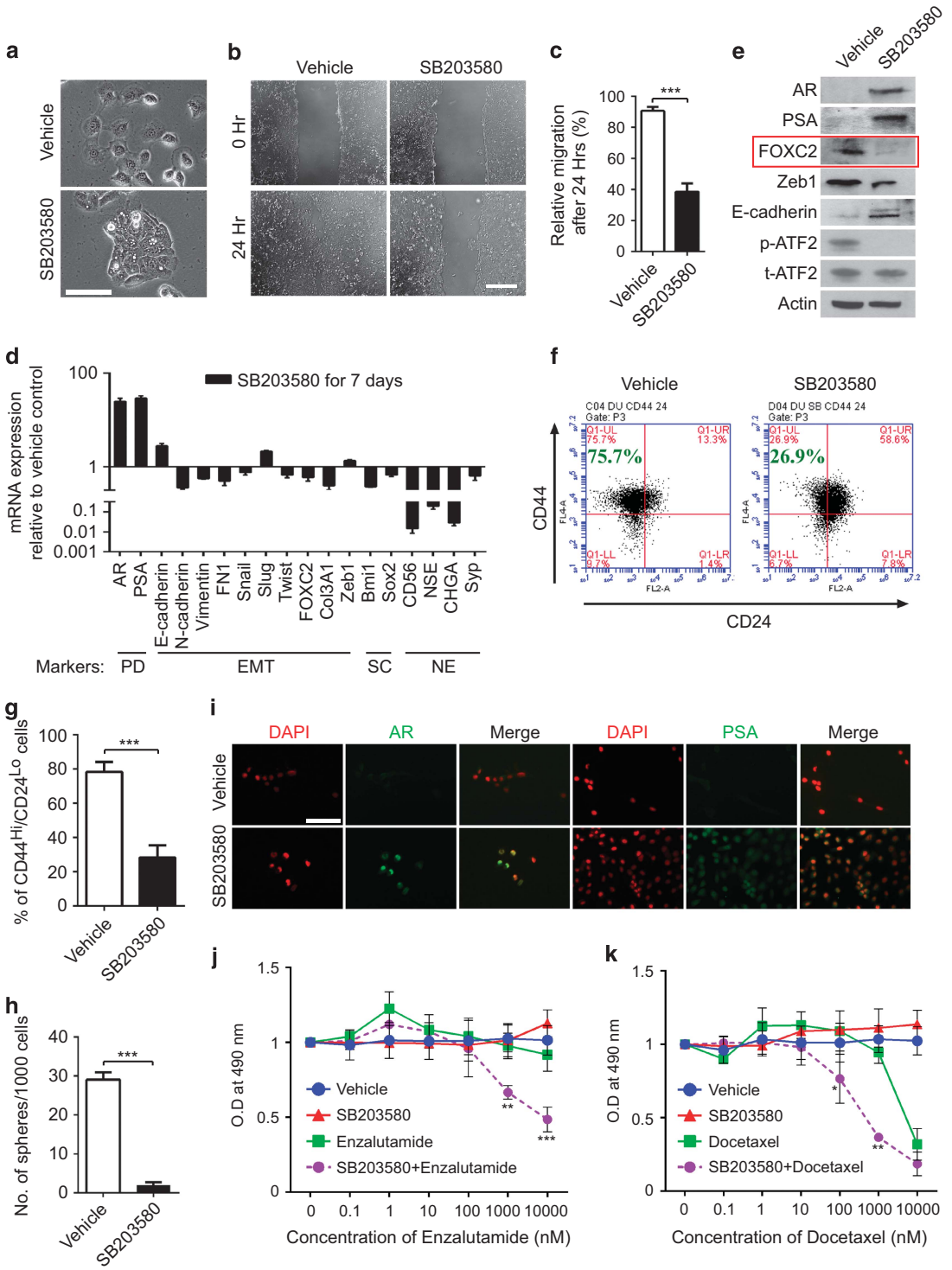

Figure 6. Suppression of p38 signaling in androgen-independent cells results in reversal of EMT, significant decrease in FOXC2-dependent stem-like properties and restoration of sensitivity to Enzalutamide and Docetaxel. (**a**) Morphology of DU145 cells on SB203580 (specific p38 signaling inhibitor) treatment for 7 days. (**b**) Representative images of wound healing assay performed with DU145 cells treated with SB203580. (**c**) Quantitation of cell migration in **b** ($n=5$; $^{***}P<0.001$; error bars indicate s.e.m.). (**d**) qRT–PCR analyses for various markers in SB203580-treated DU145 cells. *Y*-axis represents fold change in HPRT-normalized mRNA expression in SB203580-treated cells compared with vehicle-treated cells, relative to day 0 ($n=3$; error bars indicate s.e.m.). (**e**) Immunoblotting for FOXC2, key EMT markers and p38 signaling components in DU145 cells on SB203580 treatment for 7 days. (**f**) Representative FACS plots for CD44 (APC) and CD24 (PE) surface marker expression in DU145 cells treated with vehicle or SB203580 for 7 days. (**g**). Quantification of FACS analysis shown in **f** ($n=3$; error bars indicate s.e.m.; $^{***}P<0.001$). (**h**) Quantitation of tumorspheres formed per 1000 DU145 cells (treated either with vehicle or SB203580 for 7 days; $n=5$, error bars indicate s.e.m., $^{***}P<0.001$). (**i**) IF staining for AR and PSA in DU145 cells treated with vehicle or SB203580 for 7 days (scale bar = 100 μm, DAPI pseudo-colored to red). (**j** and **k**) Quantification of cell survival using MTS Assay in DU145 cells treated as indicated, with Enzalutamide (**j**) or Docetaxel (**k**). Data are represented as absorbance (OD) at 490nm ($n=3$); $^{*}P<0.05$, $^{**}P<0.01$, $^{***}P<0.001$.

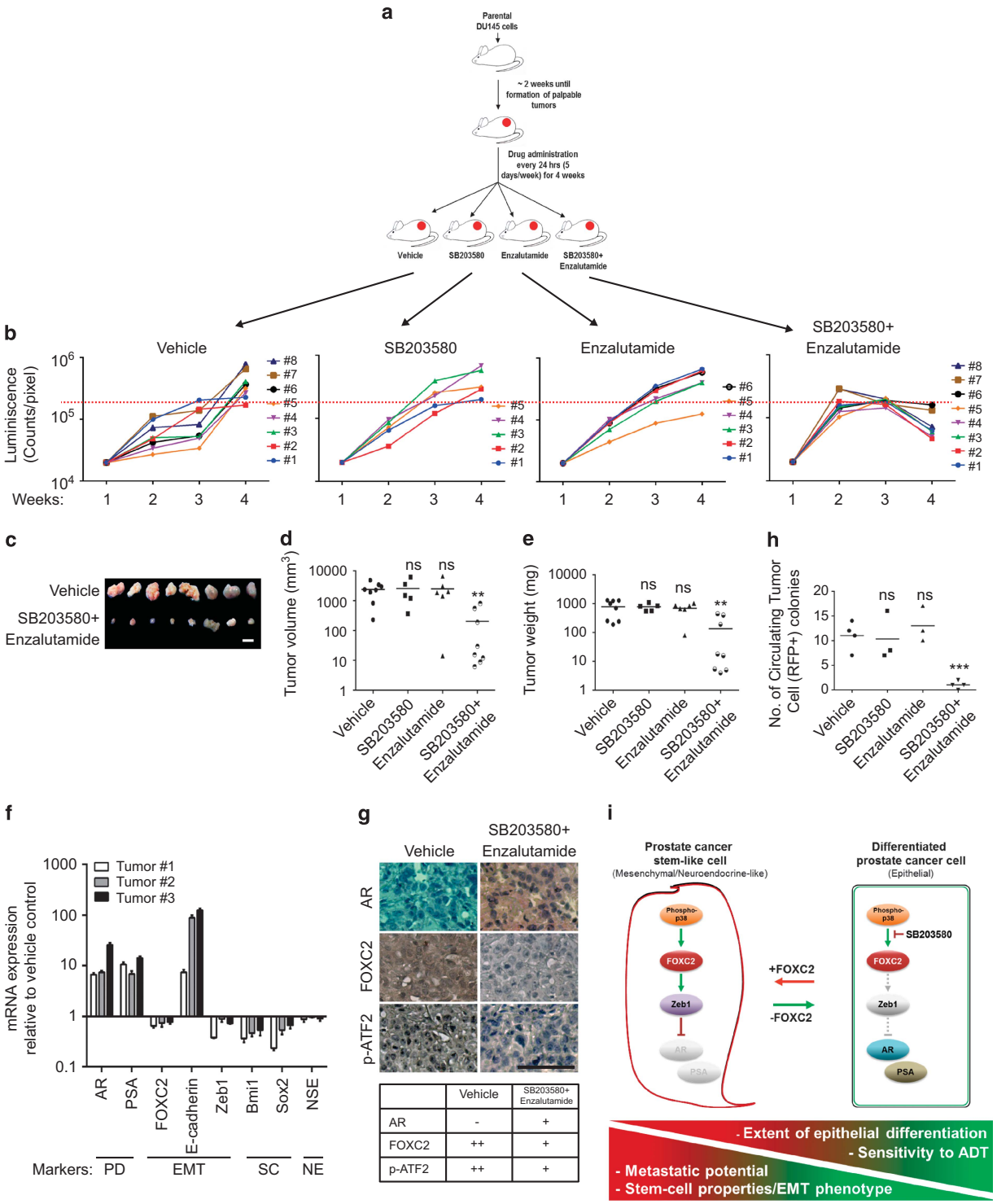

	Vehicle	SB203580+ Enzalutamide
AR	-	+
FOXC2	++	+
p-ATF2	++	+

Figure 7. Combinatorial treatment of mice bearing aggressive androgen-insensitive tumors with both SB203580 and Enzalutamide, results in significant regression of primary tumor formation as well as marked loss of circulating tumor cell population. (**a**) Schematic shows the design for *in vivo* experiments. (**b**) Quantification of luminescence of luciferase activity in tumors formed by DU145–RFP–Luciferase-labeled cells, and treated as indicated. (**c**) Tumors isolated from mice treated as indicated (scale bar,1 cm, $n = 8$ data points). (**d** and **e**). Graphs show tumor volume (**d**) and tumor weight (**e**), respectively, in indicated conditions (NS = $P > 0.05$, $^{**}P < 0.01$). (**f**) qRT–PCR analyses for FOXC2, and other indicated markers in isolated tumors. Y-axis represents fold change in HPRT-normalized mRNA expression in randomly selected tumor samples compared with that in pooled control vehicle-treated tumors ($n = 3$; error bars indicate s.e.m.). (**g**) IHC for FOXC2, AR and pATF2 (a marker for activated p38 signaling) on indicated tumors. (**h**) Quantification of colonies formed by CTCs isolated from blood of mice bearing various tumors as indicated. The colonies were confirmed to be of human origin by RFP expression that was stably introduced into DU145 cells (NS = $P > 0.05$, $^{***}P < 0.001$). (**i**) Schematic depiction of the participation of FOXC2 in the reprogramming of differentiated/epithelial PCa cells into ADT-insensitive, drug-resistant/neuroendocrine stem-like cells lacking epithelial traits. NS, not significant.

treatment in mice bearing aggressive DU145 tumors, reduced FOXC2 expression and consequent EMT/CSC/NE features, and facilitated restoration of AR/PSA expression in the tumors (Figures 7f and g).

EMT has long been recognized to provide a 'passport' to tumor cells allowing their invasion of tissue boundaries and entry into circulation. These 'altered' circulating tumor cells (CTC) then go on to sow the seeds for distant metastasis. In support of an important role for FOXC2-mediated EMT/CSC properties facilitating prostate tumor cell shedding into circulation, we indeed observed that combinatorial treatment markedly reduced the number of CTCs in mice, quantified as red fluorescent protein (RFP)-positive CTC colonies isolated from blood (Figure 7h).

DISCUSSION

Multiple recent efforts have collectively proposed that androgen depletion (the mainstay treatment for PCa) results in the induction of tumor-promoting EMT, suggesting that patients undergoing ADT might benefit from concurrent treatment with an inhibitor of EMT signaling.[13,31,32] However, effective administration of anti-EMT therapies constitutes a substantial challenge. Among the most attractive targets are EMT transcription factors (such as Snail, Twist or Zeb1).[12,33,34] Unfortunately, they are not readily 'targetable' therapeutically. Furthermore, contemporary treatment regimens, besides facilitating EMT in PCa cells, also promote adaptive tumor plasticity via NE trans-differentiation, a process that is associated with resistance to therapy, visceral metastasis and aggressive disease.[35] We therefore sought to develop an alternative method that relies on the proclivity of cancer cells to drastically alter their cellular signaling pathways to fuel growth and survival; most importantly a tangible method designed to eliminate the source/generation of PCa stem-like cells, the tumor cell subpopulation that critically determines tumor initiation, recurrence, castration-resistance and metastatic progression.

Our current studies using patient-derived prostate tissue samples as well as human PCa cell lines with differing properties of androgen-dependence and drug-resistance, establish the strong correlation between FOXC2 (a known EMT transcription factor)[17] expression and loss of AR function associated with castration-resistant prostate tumor progression. We therefore queried the possibility of using signaling inhibitors impacting FOXC2 expression/function to thwart CSC features in metastatic androgen-insensitive PCa cells. One such 'targetable' regulator of FOXC2 we have identified is the p38MAPK, a family of key serine/threonine kinases controlling cellular responses to cytokines and stress. Interestingly, the p38 signaling cascade has been previously implicated in facilitating multiple aspects of PCa progression.[36–41] p38MAPK can be effectively inhibited by small molecule therapeutics, which have already been shown to exhibit favorable activity in phase II clinical trials, for other medical conditions such as chronic obstructive pulmonary disease, cardiovascular disease and rheumatoid arthritis.[42–44] In this report, we propose a novel extension of its application to androgen-insensitive, drug-resistant PCas harboring stem-like attributes.

Intriguingly, Khandrika *et al*.[40] have reported that activation of p38 signaling in PCa cells may represent an adaptive response to hypoxic stress. Our studies done under normoxic conditions suggest that PCa cells activate p38 signaling on induction of EMT and consequent acquisition of stem-cell features, probably reflecting the early stages of transition to androgen-independence, wherein hypoxic stress is not yet pronounced. However, we predict that intervention by blockade of such a key signaling pathway leading to FOXC2-mediated stabilization of CSC attributes, is bound to be beneficial even at later stages of PCa progression, especially since invasive CTCs with stem-cell features have been detected in men with advanced metastatic CRPC.[9]

It is important to note that suppression of FOXC2 in invasive $AR^{-/lo}$ DU145 PCa cells was sufficient to restore AR expression and function, as judged by upregulation of its downstream target, PSA (Figures 3, 6 and 7). Restoration of AR/PSA expression and the associated epithelial state with loss of stem-cell functions (either using SB203580, or directly, through FOXC2 suppression) rendered these androgen-independent cells once again sensitive to Docetaxel and Enzalutamide, with substantial loss of tumorigenic NE-like features (Figures 3, 6 and 7). These observations lend further support to the view that androgens and AR demonstrate crucial tumor suppressive effects in the prostate. It is in this context that we propose the concomitant use of the p38 inhibitor, which offers the dual benefit of impeding FOXC2-mediated EMT/CSC attributes, while simultaneously restoring AR-derived protection.

In conclusion, we demonstrate that FOXC2 is an important determinant of PCa stem-cell attributes, dictating the biochemical shift to ADT- and chemo-resistance (Figure 7i). We propose a novel and tangible method to target FOXC2 functions *in vivo,* at least in part, through systemic inhibition of p38 signaling. Targeting FOXC2 curtails prostate tumor cell plasticity, by preventing both EMT, as well as NE trans-differentiation. Our future efforts will be directed to examining the molecular basis of FOXC2 function. We believe this represents a cornerstone to our understanding of the fundamental mechanisms dictating stem-cell function and tumor progression in a significant subpopulation of patients harboring variant forms of PCa (such as NEPC or small-cell prostate carcinomas) that are defined by lack of AR/PSA expression, as well as in metastatic CRPCs that arise following ADT.

MATERIALS AND METHODS

Cell lines

Authenticated LNCaP, DU145 and PC3 cells were procured from American Type Culture Collection (ATCC), Manassas, VA, USA and cultured in RPMI with 10% fetal bovine serum with penicillin/streptomycin. Cells over-expressing EMT transcription factors and short hairpin RNA (shRNA) were also cultured in the same media. HEK293T cells were cultured in DMEM with 10% fetal bovine serum and penicillin/streptomycin. All cell lines used for this study were recently confirmed negative for mycoplasma contamination. TGFβ1, LY364947 and SB203580 were used at a final concentration of 5 ng/ml, 1 μM and 5 μM, respectively.

Inhibitor experiments—cell culture

For assessing the effect of inhibition of p38MAPK signaling, cells were treated for 7 days with 5 μM SB203580[45] (EMD-Millipore, Billerica, MA, USA) dissolved in water. For assessing the combined effect of p38MAPK inhibition and the AR antagonist Enzalutamide[27,46] (SelleckChem, Houston, TX, USA) or the chemotherapeutic Docetaxel[28] (LC Laboratories, Woburn, MA, USA), cells were co-treated with SB203580 and either Enzalutamide/Docetaxel for 7 days. It is important to note that the concentration of SB203580 used to treat PCa cells in our experiments, results in selective inhibition of p38MAPK signaling, as also suggested in the study by Davies *et al*.[45] We did not observe any appreciable changes in the phosphorylation of Akt1, another potential target (data not shown).

Vectors

The use of the pCS-PSAP-EGFP-DsRed vector has been described previously.[15] pQXIP-Zeb1 was provided by Dr Harikrishna Nakshatri (Indiana University, Indianapolis, IN, USA), and pBabePuro-Snail, pBabePuro-FOXC2 and pMIG-FOXC2 by Dr Robert Weinberg (Whitehead Institute, MIT, Cambridge, MA, USA). S367E-FOXC2 and S367A-FOXC2 mutant constructs were generated by site-directed mutagenesis and subcloned into the retroviral vector MSCV-IRES–GFP. The pLKO1 lentiviral vector with shFOXC2 is previously described.[16] The pGIPZ lentiviral vectors with shSnail and shZeb1 were procured from MD Anderson shRNA Core Facility, Houston, TX, USA. Two independent shRNA sequences targeting different regions of FOXC2 5′ untranslated region were used for FOXC2 knockdown, with similar results (data shown are representative from one of them). Similarly, for shSnail and shZeb1 as well. shRNA targeting firefly

Table 1. Target sequences used in this study

Target	*shRNA sequence*
FOXC2 (#4)	5′-CCAGTGCAGCATGCGAGCGAT -3′
FOXC2 (#5)	5′-AGAACATCATGACCCTGCGAA -3′
Zeb1 (625)	5′-TAATTTGTAACGTTATTGC -3′
Zeb1 (184)	5′-TATTCTCTATCTTTTGCCG -3′
Snail (1)	5′-ACTTCTTGACATCTGAGTG -3′
Snail (2)	5′-TGTGGAGCAGGGACATTCG -3′

Abbreviation: shRNA, short hairpin RNA.

Table 2. Antibodies used in this study

Primary antibody	*Source*	*Catalog #*
β-actin	Cell Signaling Technology (Danvers, MA, USA)	4970L
AR	Santa Cruz Biotechnology (Dallas, TX, USA)	7305
E-cadherin	BD Biosciences (Franklin Lakes, NJ, USA)	610181
FN1	BD Biosciences	610077
FOXC2	Dr Nayoyuki Miura	NA
N-cadherin	BD Biosciences	610920
p38	Cell Signaling Technology	9212S
pATF2	Cell Signaling Technology	9221S
p-p38	Cell Signaling Technology	4511S
PSA	Santa Cruz Biotechnology	7638
Snail	Santa Cruz Biotechnology	28199
Total-ATF2	Cell Signaling Technology	9226S
Vimentin	Novus Biologicals (Littleton, CO, USA)	H00007431-M01
Zeb1	Santa Cruz Biotechnology	25388

Abbreviation: NA, not applicable.

Table 3. Primer sequences used in this study

Target (F/R)	*Primer sequence (5′ to 3′)*
AR-F	5'-GACGCTTCTACCAGCTCACC -3′
AR-R	5′-GCTTCACTGGGTGTGGAAAT -3′
Bmi1-F	5′- CCAGGGCTTTTCAAAAATGA-3′
Bmi1-R	5′- CCGATCCAATCTGTTCTGGT-3′
CDH1-F	5′-TGCCCAGAAAATGAAAAAGG -3′
CDH1-R	5′-GTGTATGTGGCAATGCGTTC -3′
CDH2-F	5′-GACAATGCCCCTCAAGTGTT -3′
CDH2-R	5′-CCATTAAGCCGAGTGATGGT -3′
Col3A1-F	5′-GGGAACAACTTGATGGTGCT -3′
Col3A1-R	5′- CCTCCTTCAACAGCTTCCTG-3′
FN1-F	5′-CAGTGGGAGACCTCGAGAAG -3′
FN1-R	5′-GTCCCTCGGAACATCAGAAA -3′
FOXC2-F	5′- AGAATTACTACCGGGCTGCG-3′
FOXC2-R	5′-TGAGCGCGATGTAGCTGTAG -3′
HPRT-F	5′-TGCTCGAGATGTGATGAAGG -3′
HPRT-R	5′-TCCCCTGTTGACTGGTCATT -3′
PSA-F	5′- AGTGCGAGAAGCATTCCCAA-3′
PSA-R	5′- GAAGCTGTGGCTGACCTGAA-3′
Slug-F	5′- GAGCATTTGCAGACAGGTCA-3′
Slug-R	5′-GCTTCGGAGTGAAGAAATGC -3′
Snai1-F	5′-ACCCCACATCCTTCTCACTG -3′
Snai1-R	5′-TACAAAAACCCACGCAGACA -3′
Twist1-F	5′-GGAGTCCGCAGTCTTACGAG -3′
Twist1-R	5′-CCAGCTTGAGGGTCTGAATC -3′
Vimentin-F	5′-GAGAACTTTGCCGTTGAAGC -3′
Vimentin-R	5′- TCCAGCAGCTTCCTGTAGGT-3′
Zeb1-F	5′- GCACAACCAAGTGCAGAAGA-3′
Zeb1-R	5′-CATTTGCAGATTGAGGCTGA -3′
CHGA-F	5′-TGAAATGCATCGTTGAGGTC-3′
CHGA-R	5′-ACCGCTGTGTTTCTTCTGCT-3′
SYP-F	5′-TAGGACCCAAGGTGGTCTTG-3′
SYP-R	5′-TACTCTGGAGCCCACCATTC-3′
CD56-F	5′-CGGCATTTACAAGTGTGTGG-3′
CD56-R	5′-GACATCTCGGCCTTTGTGTT-3′
NSE-F	5′-GTCCCACGTGTCTTCCACTT-3′
NSE-R	5′-CCCAAGTCAGGCCAGTTTTA-3′

luciferase (shFF3) was used as a control. Sequence details are provided in Table 1.

Isolation of CTCs

Immediately after sacrificing the mice, ~100 μl blood was isolated via venipuncture in EDTA-treated collection tubes and stored on ice. Within 30 min, the blood was spun down at 1200 r.p.m. for 5 min, and the pellet resuspended in 1 ml ACK-lysing buffer (Life Tech) and further incubated for 3–5 min. Cells were washed once with PBS, resuspended in RPMI with 10% fetal bovine serum and pen/strep, and cultured on 10-cm tissue culture dishes. RFP-positive colonies (originating from the labeled DU145 cells injected into mice) were counted after 3–4 days in culture and quantified.

Immunoblotting, immunofluorescence, RT–PCR, wound healing and tumorsphere assays

Immunoblotting, immunofluorescence, RT–PCR, wound healing and tumorsphere assays were performed as previously described.[17,47] Antibody and primer details are provided in Tables 2 and 3, respectively. Cell viability (MTS) was assessed using the CellTiter96 Aqueous One-Solution Cell Proliferation Assay kit (Promega, Fitchburg, WI, USA).

Immunohistochemistry

Human prostate tumor tissue samples representing benign prostatic hyperplasia, prostatic intraepithelial neoplasia, advanced Gleason Grade 7 and NEPC were obtained from Drs Nupam and Kiran Mahajan. Pathological evaluation was performed by two independent pathologists who agreed on the IHC scoring and the positive pattern expression of the markers. The IHC scoring *per se* was performed in a 'blinded' manner (wherein the scorers did not have access to disease classification/group allocation information) using the H-score system, including intensity (from 0 to 3+) and percentage of positive cells (from 0 to 100%), with a final scoring ranging from 0 to 300.

Flow cytometry

Fluorescence-activated cell sorting for PSA^{Hi} & $PSA^{-/lo}$ cells and $CD44^{Hi}$ & $CD24^{Lo}$ cells was performed as described previously[15,17] using BD Influx sorter (San Jose, CA, USA).

Animal experiments

Approximately 4-week-old male NOD.CB17-Prkdcscid/J mice were purchased from the Jackson Laboratory (Bar Harbor, MI, USA). All animal procedures were verified and approved by the Institutional Animal care and Use Committee of UTMDACC. To study primary prostate tumor formation, 2×10^6 RFP–luciferase-labeled DU145 cells were injected s.c. on both the flanks of 6-week-old male NOD/SCID mice. Once palpable tumors were discernable, tumor-bearing mice were randomly segregated into four groups, and drug treatment was initiated every 24 h for 5 days per week. SB203580 (0.2 μmol in 100 μl per ~20 g mouse), Enzalutamide (10 mg/kg) or a combination of both drugs (or vehicle) were administered s.c., and tumor growth was assessed as described previously.[17] Investigators were blinded to the group allocation while assessing experimental outcomes. At the end of the treatment period, tumors were excised, average diameter calculated using calipers and tumor weight noted. Tumors were then processed for RNA isolation and/or fixed in formalin, paraffin-embedded, sectioned and stained with hematoxylin/eosin and pATF2, AR and FOXC2 antibodies.

Statistical analyses

Unless otherwise stated, all samples were assayed in triplicate. All *in vitro* experiments were repeated at least three independent times, and all

animal experiments included at least 5 mice per group in each study. Unless otherwise indicated, data are represented as mean ± s.e.m., and significance was calculated using Student's unpaired two-tailed *t*-test.

CONFLICT OF INTEREST

ANP, RS, SJW, NS and SAM are inventors of a patent application in part based on findings described in this manuscript. The other authors declare no conflict of interest.

ACKNOWLEDGEMENTS

We thank Ms Neeraja Bhangre for technical assistance and Dr Sue-Hwa Lin for helpful discussions. This research was supported by grants from MDACC Prostate-SPORE, NIH R01 CA155243 and the American Cancer Society M Patricia Alexander Research Scholar award.

REFERENCES

1 Aggarwal R, Zhang T, Small EJ, Armstrong AJ. Neuroendocrine prostate cancer: subtypes, biology, and clinical outcomes. *J Natl Compr Canc Netw* 2014; **12**: 719–726.
2 Parimi V, Goyal R, Poropatich K, Yang XJ. Neuroendocrine differentiation of prostate cancer: a review. *Am J Clin Exp Urol* 2014; **2**: 273–285.
3 Niu Y, Altuwaijri S, Lai KP, Wu CT, Ricke WA, Messing EM *et al.* Androgen receptor is a tumor suppressor and proliferator in prostate cancer. *Proc Natl Acad Sci USA* 2008; **105**: 12182–12187.
4 Izumi K, Fang LY, Mizokami A, Namiki M, Li L, Lin WJ *et al.* Targeting the androgen receptor with siRNA promotes prostate cancer metastasis through enhanced macrophage recruitment via CCL2/CCR2-induced STAT3 activation. *EMBO Mol Med* 2013; **5**: 1383–1401.
5 Davis JN, Wojno KJ, Daignault S, Hofer MD, Kuefer R, Rubin MA *et al.* Elevated E2F1 inhibits transcription of the androgen receptor in metastatic hormone-resistant prostate cancer. *Cancer Res* 2006; **66**: 11897–11906.
6 Tomlins SA, Mehra R, Rhodes DR, Cao X, Wang L, Dhanasekaran SM *et al.* Integrative molecular concept modeling of prostate cancer progression. *Nat Genet* 2007; **39**: 41–51.
7 Castillo V, Valenzuela R, Huidobro C, Contreras HR, Castellon EA. Functional characteristics of cancer stem cells and their role in drug resistance of prostate cancer. *Int J Oncol* 2014; **45**: 985–994.
8 Collins AT, Berry PA, Hyde C, Stower MJ, Maitland NJ. Prospective identification of tumorigenic prostate cancer stem cells. *Cancer Res* 2005; **65**: 10946–10951.
9 Friedlander TW, Ngo VT, Dong H, Premasekharan G, Weinberg V, Doty S *et al.* Detection and characterization of invasive circulating tumor cells derived from men with metastatic castration-resistant prostate cancer. *Int J Cancer* 2014; **134**: 2284–2293.
10 Patrawala L, Calhoun T, Schneider-Broussard R, Li H, Bhatia B, Tang S *et al.* Highly purified CD44+ prostate cancer cells from xenograft human tumors are enriched in tumorigenic and metastatic progenitor cells. *Oncogene* 2006; **25**: 1696–1708.
11 Santoni M, Conti A, Burattini L, Berardi R, Scarpelli M, Cheng L *et al.* Neuroendocrine differentiation in prostate cancer: novel morphological insights and future therapeutic perspectives. *Biochim Biophys Acta* 2014; **1846**: 630–637.
12 Li P, Wang J, Chu M, Zhang K, Yang R, Gao WQ. Zeb1 promotes androgen independence of prostate cancer via induction of stem cell-like properties. *Exp Biol Med (Maywood)* 2014; **239**: 813–822.
13 Sun Y, Wang BE, Leong KG, Yue P, Li L, Jhunjhunwala S *et al.* Androgen deprivation causes epithelial-mesenchymal transition in the prostate: Implications for androgen- deprivation therapy. *Cancer Res* 2012; **72**: 527–536.
14 Zhu ML, Kyprianou N. Role of androgens and the androgen receptor in epithelial-mesenchymal transition and invasion of prostate cancer cells. *FASEB J* 2010; **24**: 769–777.
15 Qin J, Liu X, Laffin B, Chen X, Choy G, Jeter CR *et al.* The PSA(-/lo) prostate cancer cell population harbors self-renewing long-term tumor-propagating cells that resist castration. *Cell Stem Cell* 2012; **10**: 556–569.
16 Mani SA, Yang J, Brooks M, Schwaninger G, Zhou A, Miura N *et al.* Mesenchyme Forkhead 1 (FOXC2) plays a key role in metastasis and is associated with aggressive basal-like breast cancers. *Proc Natl Acad Sci USA* 2007; **104**: 10069–10074.
17 Hollier BG, Tinnirello AA, Werden SJ, Evans KW, Taube JH, Sarkar TR *et al.* FOXC2 expression links epithelial-mesenchymal transition and stem cell properties in breast cancer. *Cancer Res* 2013; **73**: 1981–1992.
18 Paranjape AN, Balaji SA, Mandal T, Krushik EV, Nagaraj P, Mukherjee G *et al.* Bmi1 regulates self-renewal and epithelial to mesenchymal transition in breast cancer cells through Nanog. *BMC Cancer* 2014; **14**: 785.
19 Wellner U, Schubert J, Burk UC, Schmalhofer O, Zhu F, Sonntag A *et al.* The EMT-activator ZEB1 promotes tumorigenicity by repressing stemness-inhibiting microRNAs. *Nat Cell Biol* 2009; **11**: 1487–1495.
20 Chaffer CL, Marjanovic ND, Lee T, Bell G, Kleer CG, Reinhardt F *et al.* Poised chromatin at the ZEB1 promoter enables breast cancer cell plasticity and enhances tumorigenicity. *Cell* 2013; **154**: 61–74.
21 Pulukuri SM, Gondi CS, Lakka SS, Jutla A, Estes N, Gujrati M *et al.* RNA interference-directed knockdown of urokinase plasminogen activator and urokinase plasminogen activator receptor inhibits prostate cancer cell invasion, survival, and tumorigenicity in vivo. *J Biol Chem* 2005; **280**: 36529–36540.
22 Hurt EM, Kawasaki BT, Klarmann GJ, Thomas SB, Farrar WL. CD44+ CD24(-) prostate cells are early cancer progenitor/stem cells that provide a model for patients with poor prognosis. *Br J Cancer* 2008; **98**: 756–765.
23 Hollier BG, Evans K, Mani SA. The epithelial-to-mesenchymal transition and cancer stem cells: a coalition against cancer therapies. *J Mammary Gland Biol Neoplasia* 2009; **14**: 29–43.
24 Tzelepi V, Zhang J, Lu JF, Kleb B, Wu G, Wan X *et al.* Modeling a lethal prostate cancer variant with small-cell carcinoma features. *Clin Cancer Res* 2012; **18**: 666–677.
25 Aparicio A, Tzelepi V, Araujo JC, Guo CC, Liang S, Troncoso P *et al.* Neuroendocrine prostate cancer xenografts with large-cell and small-cell features derived from a single patient's tumor: morphological, immunohistochemical, and gene expression profiles. *Prostate* 2011; **71**: 846–856.
26 Taube JH, Herschkowitz JI, Komurov K, Zhou AY, Gupta S, Yang J *et al.* Core epithelial-to-mesenchymal transition interactome gene-expression signature is associated with claudin-low and metaplastic breast cancer subtypes. *Proc Natl Acad Sci USA* 2010; **107**: 15449–15454.
27 Balbas MD, Evans MJ, Hosfield DJ, Wongvipat J, Arora VK, Watson PA *et al.* Overcoming mutation-based resistance to antiandrogens with rational drug design. *eLife* 2013; **2**: e00499.
28 Tamaki H, Harashima N, Hiraki M, Arichi N, Nishimura N, Shiina H *et al.* Bcl-2 family inhibition sensitizes human prostate cancer cells to docetaxel and promotes unexpected apoptosis under caspase-9 inhibition. *Oncotarget* 2014; **5**: 11399–11412.
29 Koul HK, Pal M, Koul S. Role of p38 MAP kinase signal transduction in solid tumors. *Genes Cancer* 2013; **4**: 342–359.
30 Shiota M, Zardan A, Takeuchi A, Kumano M, Beraldi E, Naito S *et al.* Clusterin mediates TGF-beta-induced epithelial-mesenchymal transition and metastasis via Twist1 in prostate cancer cells. *Cancer Res* 2012; **72**: 5261–5272.
31 Li P, Yang R, Gao WQ. Contributions of epithelial-mesenchymal transition and cancer stem cells to the development of castration resistance of prostate cancer. *Mol Cancer* 2014; **13**: 55.
32 Marin-Aguilera M, Codony-Servat J, Reig O, Lozano JJ, Fernandez PL, Pereira MV *et al.* Epithelial-to-mesenchymal transition mediates docetaxel resistance and high risk of relapse in prostate cancer. *Mol Cancer Ther* 2014; **13**: 1270–1284.
33 McKeithen D, Graham T, Chung LWK, Odero-Marah V. Snail transcription factor regulates neuroendocrine differentiationin LNCaP prostate cancer cells. *Prostate* 2010; **70**: 982–992.
34 Kwok WK, Ling MT, Lee TW, Lau TC, Zhou C, Zhang X *et al.* Up-regulation of TWIST in prostate cancer and its implication as a therapeutic target. *Cancer Res* 2005; **65**: 5153–5162.
35 Nouri M, Ratther E, Stylianou N, Nelson CC, Hollier BG, Williams ED. Androgen-targeted therapy-induced epithelial mesenchymal plasticity and neuroendocrine transdifferentiation in prostate cancer: an opportunity for intervention. *Front Oncol* 2014; **4**: 370.
36 Shida Y, Igawa T, Hakariya T, Sakai H, Kanetake H. p38MAPK activation is involved in androgen-independent proliferation of human prostate cancer cells by regulating IL-6 secretion. *Biochem Biophys Res Commun* 2007; **353**: 744–749.
37 Milone MR, Pucci B, Bruzzese F, Carbone C, Piro G, Costantini S *et al.* Acquired resistance to zoledronic acid and the parallel acquisition of an aggressive phenotype are mediated by p38-MAP kinase activation in prostate cancer cells. *Cell Death Dis* 2013; **4**: e641.
38 Ricote M, Garcia-Tunon I, Fraile B, Fernandez C, Aller P, Paniagua R *et al.* P38 MAPK protects against TNF-alpha-provoked apoptosis in LNCaP prostatic cancer cells. *Apoptosis* 2006; **11**: 1969–1975.
39 Gan L, Wang J, Xu H, Yang X. Resistance to docetaxel-induced apoptosis in prostate cancer cells by p38/p53/p21 signaling. *Prostate* 2011; **71**: 1158–1166.

40 Khandrika L, Lieberman R, Koul S, Kumar B, Maroni P, Chandhoke R *et al.* Hypoxia-associated p38 mitogen-activated protein kinase-mediated androgen receptor activation and increased HIF-1alpha levels contribute to emergence of an aggressive phenotype in prostate cancer. *Oncogene* 2009; **28**: 1248–1260.
41 Ma B, Wells A. The mitogen-activated protein (MAP) kinases p38 and extracellular signal-regulated kinase (ERK) are involved in hepatocyte-mediated phenotypic switching in prostate cancer cells. *J Bol Chem* 2014; **289**: 11153–11161.
42 Cohen S, Fleischmann R. Kinase inhibitors: a new approach to rheumatoid arthritis treatment. *Curr Opin Rheumatol* 2010; **22**: 330–335.
43 MacNee W, Allan RJ, Jones I, De Salvo MC, Tan LF. Efficacy and safety of the oral p38 inhibitor PH-797804 in chronic obstructive pulmonary disease: a randomised clinical trial. *Thorax* 2013; **68**: 738–745.
44 Cheriyan J, Webb AJ, Sarov-Blat L, Elkhawad M, Wallace SM, Maki-Petaja KM *et al.* Inhibition of p38 mitogen-activated protein kinase improves nitric oxide-mediated vasodilatation and reduces inflammation in hypercholesterolemia. *Circulation* 2011; **123**: 515–523.
45 Davies SP, Reddy H, Caivano M, Cohen P. Specificity and mechanism of action of some commonly used protein kinase inhibitors. *Biochem J* 2000; **351**: 95–105.
46 Scher HI, Fizazi K, Saad F, Taplin ME, Sternberg CN, Miller K *et al.* Increased survival with enzalutamide in prostate cancer after chemotherapy. *N Engl J Med* 2012; **367**: 1187–1197.
47 Sarkar TR, Battula VL, Werden SJ, Vijay GV, Ramirez-Pena EQ, Taube JH *et al.* GD3 synthase regulates epithelial-mesenchymal transition and metastasis in breast cancer. *Oncogene* 2015; **34**: 2958–2967.

Supplementary Information accompanies this paper on the Oncogene website (http://www.nature.com/onc)